

## Epitaxial Growth and Atomic-Scale Investigation of Dielectric $\text{Ca}_{1.46}\text{Nb}_{1.11}\text{Ti}_{1.38}\text{O}_7$ Thin Films

Xiao-Wei Jin<sup>1</sup>, Yue-Hua Chen<sup>2</sup>, Lu Lu<sup>1</sup>, Shao-Bo Mi<sup>3</sup>, Hong Wang<sup>1,3</sup> and Chun-Lin Jia<sup>1,3,4</sup>

<sup>1</sup>. The School of Electronic and Information Engineering, Xi'an Jiaotong University, Xi'an, PR China.

<sup>2</sup>. Key Laboratory for Organic Electronics and Information Displays & Institute of Advanced Materials, Nanjing University of Posts & Telecommunications, Nanjing, PR China.

<sup>3</sup>. State Key Laboratory for Mechanical Behavior of Materials, Xi'an Jiaotong University, Xi'an, PR China.

<sup>4</sup>. Peter Grünberg Institute and Ernst Ruska Center for Microscopy and Spectroscopy with Electrons, Forschungszentrum Jülich, Jülich, Germany.

Pyrochlore-based dielectric ceramics with the stoichiometry of  $\text{A}_2\text{B}_2\text{O}_7$  have attracted much attention in recent years as the promising candidates for tunable microwave devices, such as capacitors, phase shifters, filters and coplanar waveguides, due to their high permittivity, low dielectric loss, high thermal stability and high tunability [1-2]. In addition, they can be applied as photocatalysts for water splitting [3]. Recently, Roth et al. reported that by the traditional solid state reaction method a single pyrochlore-phase can be obtained for the stoichiometry of  $\text{Ca}_{1.46}\text{Nb}_{1.11}\text{Ti}_{1.38}\text{O}_7$  (CNT) [4]. It is well known that the structural and physical properties of thin films are often different from those of bulk materials due to the influence of the substrates [5-6]. In contrast to the studies on the structural and physical properties of CNT bulk [4], the growth and structural properties of CNT films were seldom reported.

In this work, we successfully fabricated the CNT thin films on [110]-oriented  $\text{NdGaO}_3$  (NGO) substrates at 900°C using the high-pressure sputtering system. The oxygen flowing pressure was 2 mbar. The crystallinity of the CNT films was characterized by high-resolution X-ray diffraction (XRD) using PANalyticalX'Pert MRD. Cross-sectional (S)TEM samples were prepared by focused ion beam (FIB) technique (FEI Dual beam Helios NanoLab 600i). Bright-field (BF) TEM images and selected area electron diffraction (SAED) patterns were acquired by a JEOL 2100 transmission electron microscope. Atomic-resolution high-angle annular dark field (HAADF) and annular bright field (ABF) imaging were performed on a JEOL ARM200F with a probe aberration corrector, operated at 200 kV.

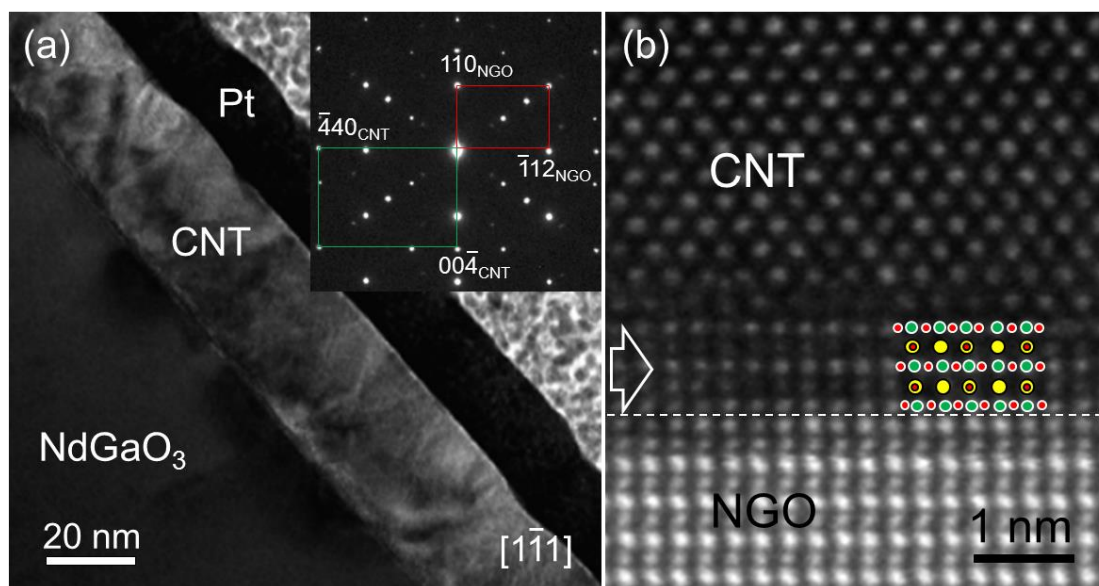
Figure 1(a) shows a low-magnification BF-TEM image and the corresponding SAED pattern of the CNT/NGO(110) heterostructure, recorded along the [1-11] zone axis of NGO. In the BF-TEM image, the film-substrate interface can be easily distinguished due to the contrast difference between the films and the substrates, and the thickness of the films is determined as about 28 nm. No interfacial dislocations are observed at the film-substrate interface. Contrast variation in the films indicates that the CNT films exhibit a columnar structure. In the SAED pattern, two sets of diffraction spots resulting from CNT and NGO are denoted by a green and a red rectangle, respectively. The SAED pattern illustrates that the CNT films have a face-centered cubic structure. The crystalline orientation relationship between the films and the substrates can be determined as  $[001](010)_{\text{CNT}}//[110](001)_{\text{NGO}}$ .

Figure 1(b) displays an atomic-resolution HAADF-STEM image of the CNT/NGO(110) heterostructure, viewed along the [1-11] zone axis of the substrates. The surface plane of the substrates is indicated by a horizontal white broken-line. Based on HAADF and SAED results, the CNT films have a cubic-pyrochlore structure with the lattice parameter of about 1.02 nm. Additionally, a buffer layer with a

thickness of about 1 nm is observed between the CNT films and the substrates, as denoted by a horizontal white arrow. The A-type and B-type atomic columns in the buffer layer are indicated by yellow circles and green circles, respectively. In combination with the corresponding ABF-STEM image, the positions of oxygen columns are determined, as denoted by the red circles. The buffer layer has a perovskite-type structure, which coherently grows on the NGO substrates. Considering the large lattice mismatch between CNT and NGO (~11.89%), the formation of the buffer layer may result from the substrate-induced strains and the composition fluctuation in the initial state of the film growth, which is in favor of the epitaxial growth of the CNT films on the NGO(110) substrates [7].

#### References:

- [1] A Le Febvrier *et al*, ACS Appl. Mater. & Interfaces **4** (2012), p. 5227.  
 [2] X Yan *et al*, Ferroelectr. **406** (2010), p. 3.  
 [3] Z Shao *et al*, J. Mater. Chem. **22** (2012), p. 9806.  
 [4] RS Roth *et al*, J. Solid State Chem. **181** (2008), p. 406.  
 [5] XW Jin *et al*, J. Alloys Compd. **676** (2016), p. 173.  
 [6] XW Jin *et al*, Appl. Phys. Lett. **109** (2016), p. 031904.  
 [7] The work was supported by the National Basic Research Program of China (No. 2015CB654903) and the National Natural Science Foundation of China (Nos. 51471169 and 51390472).



**Figure 1.** (a) A low-magnification BF-TEM image and the corresponding SAED pattern of the CNT/NGO(110) heterojunction, recorded along the [1-11] zone axis of NGO. (b) An atomic-resolution HAADF image of the CNT/NGO(110) heterostructure viewed along the [1-11] zone axis of the substrates. The white broken-line denotes the interface between the buffer layer and the substrates, and the horizontal white arrow denotes the buffer layer. Yellow circles, green circles and red circles denote the A-type columns, the B-type columns and the oxygen columns in the buffer layer, respectively.